

NASA TM X-55586

THE NEUTRAL SHEET IN THE GEOMAGNETIC TAIL: ITS MOTION, EQUIVALENT CURRENTS, AND FIELD LINE CONNECTION THROUGH IT

GPO PRICE \$ _____

CFSTI PRICE(S) \$ _____

Hard copy (HC) \$2.00

Microfiche (MF) .50

BY

T. W. SPEISER
N. F. NESS

ff 653 July 65

N67 11364

FACILITY FORM 802

(ACCESSION NUMBER)

38

(PAGES)

TMX-55586

(NASA CR OR TMX OR AD NUMBER)

(THRU)

1

(CODE)

13

(CATEGORY)

JUNE 1966



GODDARD SPACE FLIGHT CENTER
GREENBELT, MD.

THE NEUTRAL SHEET IN THE GEOMAGNETIC TAIL:
ITS MOTION, EQUIVALENT CURRENTS, AND FIELD LINE
CONNECTION THROUGH IT

by

T. W. Speiser

and

N. F. Ness

JUNE 1966

THE NEUTRAL SHEET IN THE GEOMAGNETIC TAIL:
ITS MOTION, EQUIVALENT CURRENTS, AND FIELD
LINE CONNECTION THROUGH IT

by

T. W. Speiser

and

N. F. Ness

N67-11364
Abstract

From March 22 to May 26, 1964, during orbits 30 through 47, the Imp-1 satellite was located within the earth's magnetic tail and measurements of the imbedded neutral sheet were possible. Forty-two observations of magnetic field reversals accompanied by a decrease in the field magnitude were detected. Of these, 38 are identified as crossings of a well developed magnetic neutral sheet or current sheet. The relatively thin neutral sheet lies within a broad region of magnetic field depression and plasma enhancement, or "plasma sheet". The neutral sheet frequently appears to be moving relative to the satellite with a maximum velocity of a few kilometers per second and on many orbits multiple crossings occur. The formation of the sheet appears to begin near the magnetic equatorial plane at a geocentric distance of $10 \pm 3R_E$. The sheet thickness appears to be larger close to the Earth and the dawn side of

↓
over

the tail and smaller farther away and toward the noon-midnight meridian. At its thinnest region the sheet appears to be about 500 km thick and about 5000 km at the thickest part. The normal component of magnetic field within the sheet appears from these measurements to be 1 to 4 gammas toward the dawn side of the tail and less than 1 gamma near the noon-midnight meridian plane.

Author

Introduction

With the discovery of an interplanetary magnetic field, Dungey [1961] suggested a geomagnetic field model incorporating neutral points in the combined earth-dipole and interplanetary field. Earlier work [Giovanelli, 1947, Hoyle, 1949, Dungey, 1953] had suggested the possibility of particle acceleration at magnetic neutral points. Thus the neutral point model was proposed as a near earth source of accelerated auroral particles as opposed to the sun and subsequent direct propagation. For such a model, the magnetic field should collapse to a sheet-like configuration near the neutral points with the field direction reversing across the sheet and the magnitude being relatively very weak within the sheet itself. Previous reports using data from the IMP-1 satellite have discussed the observed magnetic field topology in the magnetosphere, correlations of energetic particles and magnetic field data, the interplanetary medium, and the discovery of a magnetically neutral sheet in the magnetospheric tail [Ness, 1965; Behannon and Ness, 1966; Ness and Williams, 1966; Anderson and Ness, 1966; Williams and Ness, 1966].

The neutral sheet has been previously defined [Ness, 1965] as a region of abrupt directional change in the earth's magnetic tail field, where the magnitude decreases to a very small value. The magnitude of field minimum is not found to be identically zero, however, so the neutral sheet is not ideally "neutral".

Since the field magnitude does decrease in the neutral sheet, the hypothesis of a purely rotational discontinuity in the magnetic field is not supported by the data.

The neutral sheet identified from the above definition should be distinguished from the broad region of magnetic field depression associated with the large fluxes of high energy electrons found with measurements on Imp-1 [Anderson and Ness, 1966]. This broad region, of the order of 5-10 R_E in thickness, probably corresponds to the plasma sheet identified from measurements on the Vela satellite [Bame et al., 1966]. In this context then, the neutral sheet discussed in this report is that relatively narrow region of field reversal found within the plasma sheet region.

From orbits 30 through 47, March 22 to May 26, 1964, the Imp-1 satellite was within the earth's magnetic tail. The neutral sheet, or a sheet-like crossing, has been detected on all of these 18 orbital passes in the tail. Multiple crossings are often observed, and a total of 42 crossings have been analyzed. Of these, the first four (orbits 30-33) occur within 15 R_E (earth-radii), and appear to be representative of extended or inflated field lines near the dawn side of the magnetosphere, without as much of a sheet-like character as the later crossings. The multiple crossings can be explained by assuming that the sheet is moving back and forth across the position of the satellite. The sheet thickness cannot be uniquely determined for any given crossing unless the sheet velocity is known, because of the problem of space-time

separation. However, the average thickness can be estimated by assuming that the average sheet velocity observed on many crossings can reasonably be expected to be close to zero. The detailed magnetic field measurements within and near the neutral sheet are investigated in this report. From the change in the magnetic field on crossing the sheet, the equivalent current per unit length is computed from the curl of the vector field. The general flow pattern is across the tail from dawn to dusk with a significant component down the tail for those sheet crossings near the earth and toward the dawn side.

The strength of the magnetic field within and normal to the sheet is also measured. It is important to know the value of this component in order to distinguish between models of the magnetospheric tail with "open" or "closed" field topologies. These Imp-1 results indicate a normal component of the order of 10-20% of the tail field beyond about $15 R_E$ near the dawn meridian, with a smaller normal component of about 5% or less toward the noon-midnight meridian plane. It thus appears that there is some connection of northern and southern hemispheric field lines across the geomagnetic tail during these measurements of Imp-1. However, it is not possible to say unambiguously whether or not the vicinity of a neutral point or line was reached. The answer to this important question will have to await additional measurements and especially those farther into the tail.

From these projections, the magnetic field appears to have a dipole character as seen for $X_{sm}, Z_{sm} < 5 R_E$, but because the orbit distribution is spatially biased, the available samples tend to avoid low magnetic latitudes close to the earth. Multiple reversals are evident as seen for $-1 < Y_{sm} < +1$, although many sheet crossings and other details cannot be observed because of the hourly averaging which has been performed.

Figure 4 shows a plot of Z_{sm} and Z_{mag} at the neutral sheet crossing position as a function of geocentric distance where Z_{mag} is the perpendicular distance from the dipole equatorial plane. The orbit number and the value of χ_{ss} , the geomagnetic latitude of the subsolar point, is given for the crossings. If the solar-magnetospheric equatorial plane precisely described the position of the neutral sheet, then all of these points would fall on $Z_{sm} = 0$. However, if one imagines that the neutral sheet begins near the geomagnetic equatorial plane at some fixed geocentric distance, then as the dipole equatorial plane tilts or wobbles with respect to the solar ecliptic plane, the neutral sheet will move above or below as the solar wind forms the geomagnetic tail. The neutral sheet termination thus occurs on the magnetic equatorial plane at that distance where "closed" field lines forming the magnetosphere are separated from field lines extended into the tail. "Closed" in this sense means field lines which may be inflated, but on which stable trapping can still occur, as defined by conservation of the adiabatic invariants. Serlemitsos [1966] has clearly

indicated a distinction between this type of closed field line and "tail" field lines. He finds the boundary between these lines on quiet days to extend to distances beyond $12 R_E$, but to decrease rapidly with increasing magnetic activity.

T. Murayama (Private communication, 1966) has suggested the use of a distance $R_o = Z_{sm} / \sin \chi_{ss}$, for the ordering of the neutral sheet crossings. This distance is determined from the position of the point separating the closed and extended field lines mentioned above, if the neutral sheet is parallel to the solar-magnetospheric equatorial plane in the tail. R_o , calculated from the points presented in Figure 4, is found to be approximately $10 R_E$ with an RMS deviation of $\pm 3 R_E$ for those crossings within $\pm 6 R_E$ of the noon-midnight meridian plane (orbits 41 through 47).

For the earlier neutral sheet crossings, R_o appears to be smaller, although there are obviously some anomalous points, such as orbit 37, where Z_{sm} is negative and χ_{ss} is positive. Those crossings where χ_{ss} is very small do not give a meaningful numerical result for R_o . Although R_o has meaning for all values of χ_{ss} , from observations of neutral sheet crossings R_o can only be determined from the above equation when $\chi_{ss} > 2-5^\circ$.

A sketch indicating the possible configuration of the neutral sheet with magnetic field lines is given as Figure 5. The projected magnetic field vectors for $-1 < Y_{sm} < 1$, from Figure 3 are included. Positions where neutral surface crossings have been found near this meridian plane are indicated, although the

value of χ_{s_s} used for this drawing (25°) is not correct for all of the indicated crossings (see Figure 4).

A possible neutral surface configuration passing near these observed crossings is indicated. The extended field lines are drawn in to agree in general with the measured hourly averages, although the vectors near the sheet around $24 R_E$ do not display the correct sense for this specific configuration. The reason for this is that the vectors in this region were averaged over hours with χ_{s_s} different than 25° .

The extended field lines sketched in Figure 5 represent the picture of a real field weaker than the undistorted geomagnetic field close to the Earth, somewhat uniform and reversing across the neutral sheet farther out, with some field lines crossing the sheet. Configurations such as purely "inflated" field lines, disconnected field lines, and field lines with no reverse curvature could be proposed.

Purely "inflated" field lines would not, however, be consistent with the vector field as presented in Figures 1, 2 and 3, or with the evidence of the field magnitude going through a rather sharp minimum at a neutral sheet crossing. Disconnected field lines (a strictly neutral sheet) would not be consistent with the evidence of a non-zero normal field component at the center of the sheet. (See the next section, Figure 9). Field lines extended, but with no reverse curvature (reverse curvature being a condition necessitating

external plasma pressure), would imply a weaker field below the neutral sheet than above it for the case of a large positive value of χ_{ss} as drawn in Figure 5. There seems to be insufficient evidence to support or deny this latter possibility from the data since the satellite spends a disproportionate amount of time below the sheet and thus the satellite does not provide adequate sampling of the field above the sheet.

Detailed Observations of the Fields Within the Neutral Sheet.

The Imp-1 magnetic field data consisting of 12 vector measurements every 5 minutes has been plotted for times near a neutral sheet crossing for orbits 30 through 47. In the data a neutral sheet crossing is determined at that time interval when the magnetic field reverses from a generally anti-solar to solar direction, or vice-versa with an accompanying decrease in the field magnitude. The presence of plasma in the tail can reduce the magnetic field strength by its diamagnetic effect [Anderson and Ness, 1966] but cannot cause the magnetic field to reverse directions, unless the plasma is assumed to have a magnetic field "frozen-in" of exactly the right character. For the many observed neutral-sheet crossings, this assumption would appear to introduce an unnecessary complication so the determination of a neutral sheet crossing will be made as described above.

Figure 6 is a sample plot of magnetic field data on orbit 45 from 2100 May 18 to 0150 UT May 19, 1964. The total field (\bar{F}) and the solar-magnetospheric

X, Y and Z components are plotted for this time interval. Each point in Figure 6 is an average of 12 measurements over an interval of 5.46 minutes.

Previous plots [Ness et al. 1964, Ness, 1965] of $(\bar{F}, \theta, \phi)_{SE}$ have been presented. In those plots neutral sheet crossings were identified as regions with abrupt reversals in ϕ with an accompanying decrease in \bar{F} .

From component plots such as in Figure 6, neutral sheet crossings are identified by a change in sign of B_x accompanied by a minimum in \bar{F} . Five crossings are seen for this time interval on orbit 45. The crossing times, indicated on the plot, are not as short as would be concluded from the ϕ_{SE} reversals alone.

Several interpretations of this data are possible. The satellite may be crossing several sheets with varying thicknesses at about the same satellite-sheet relative velocity; it may be crossing several sheets with about the same thickness but varying relative velocities, or the satellite may be crossing only one sheet which is moving back and forth across the position of the satellite in response to varying solar wind characteristics. The most direct interpretation appears to be the latter and an important point in favor of this hypothesis is the occurrence of only a single crossing on orbits 41 and 42.

If the plane of the neutral sheet were identified, then the magnetic field component perpendicular to the sheet would not change on crossing the sheet. From Figure 6 we see that although B_z is fairly constant and close to zero,

there is a slight oscillation (the amplitude is about 2 gammas) which is out of phase with the oscillation in B_x . A rotation of 5 degrees about the Y_{sm} axis is found to decrease the amplitude of oscillation of B_z by about 50%. Thus for this particular time, the neutral sheet locally appears to be tipped down by about 5° from solar-magnetospheric coordinates with respect to the earth-sun direction.

Similar rotations have been made on many of the other sheet crossings, and it is found that the local plane of the neutral surface as measured at the point of crossing is usually parallel to the solar magnetospheric equatorial plane to within about $\pm 10^\circ$.

Figure 7 is a plot of data from orbit 32 near a neutral sheet crossing. The geocentric distance for the crossing is $10.35 R_e$, and only one crossing is made. The sheet traversal time of 98 minutes is considerably larger than those times for orbit 45. Note also the obvious differences between Figures 5 and 6 in the change in B_y across the sheet and the large value of B_z in the sheet.

Plots similar to Figures 6 and 7 have been made for each of the 18 orbits of Imp-1 in the tail. Individual 20 second data points have been used in general although the 5.46 minute averages are shown in Figures 6 and 7 for clarity of presentation. The fields in the tail vary so smoothly with time in general, that it makes little difference for the analysis of equivalent currents and normal components whether the averages or the individual points are used.

Equivalent Currents.

Once the plane of the neutral sheet has been found, curl \mathbf{B} and thus the equivalent current density can be computed as follows. The time rate of change of a field component B_i is

$$\frac{dB_i}{dt} = \frac{\partial B_i}{\partial t} + (\mathbf{V} \cdot \nabla) B_i \quad (1)$$

It will be assumed that the B_i do not change explicitly with time over the interval of a sheet crossing, and that only partial derivatives with respect to Z exist. This assumption implies that the sheet is two dimensional and stationary in time except for possible spatial motion. Therefore,

$$\frac{dB_i}{dt} = V_z \frac{\partial B_i}{\partial z}$$

where V_z is the relative velocity between the satellite and sheet. Using

$\nabla \times \mathbf{B} = \mu_0 \mathbf{J}'$ (mks units are used) we have

$$\left[J'_x, J'_y, J'_z \right] = \frac{1}{\mu_0 V_z} \left[-\frac{dB_y}{dt}, \frac{dB_x}{dt}, 0 \right]$$

A straight line fit to the data on the sheet crossings is indicated in the (B_x, B_y, B_z) plots of Figures 6 and 7. Since the IMP-1 satellite initially approaches the neutral sheet from below ($-z$ values) the relative velocity should have the same sign as dB_x/dt . The relative velocity, V_z multiplied by the time taken to cross the sheet, Δt , should give the sheet thickness, T . Thus,

$$V_z = (T/\Delta t) \cdot (\text{sign of } dB_x/dt)$$

\mathbf{J}' is the current/area, so that multiplying by the sheet thickness yields the current/length, \mathbf{J} .

$$J_x = -\mu_o \Delta B_y \cdot (\text{sign of } \Delta B_x)$$

$$J_y = \mu_o^{-1} |\Delta B_x|$$

$$J_z = 0$$

\mathbf{J} is therefore independent of the relative velocity and the sheet thickness, and knowledge of either V_z or T would be sufficient to specify the other. The accuracy of measurement of \mathbf{J} is $\pm 10\text{-}20\%$, the errors due to the uncertainty in the straight line fitting of the data.

Figure 8 shows \mathbf{J} as a function of the crossing position in the solar-magnetospheric coordinate system, for orbits 30 through 47. The currents have been calculated from the data in solar-magnetospheric coordinates, so insofar as the neutral surface is tipped slightly from these coordinates, a slight error is introduced. Also because of a slight tipping, J_z in solar-magnetospheric coordinates may have a small non-zero value which is not considered here.

Multiple crossings are seen in Figure 8 as separate current vectors at different positions for the same orbit number. Thus orbit 35 has two crossings, orbit 36, three crossings etc. Orbit 45 has 5 crossings beyond $25 R_e$ (see also Figure 6), and three crossings within $20 R_e$. Similarly orbit 44 has three crossings beyond $25 R_e$ and three within $20 R_e$. Since the solar-magnetospheric equatorial plane ($Z_{sm} = 0$) wobbles daily, there are orbits of IMP-1 in which the satellite comes close to or crosses $Z_{sm} = 0$ two or more times each orbital period (93.5 hours). Behannon and Ness in Figure 7 (1966) show this characteristic feature of the data. Thus the separation of the neutral sheet crossings in orbits 44 and 45 into two groups (beyond $25 R_e$ and within $20 R_e$) is due to the diurnal wobbling of the neutral sheet.

It should be noticed that the currents close to the earth and near the dawn edge of the tail (orbits 30-33) have large components down the tail, and that the vector current tends to be dominantly across the tail as geocentric distance increases. The magnitude of the current is largest for the first four crossings, but subsequently no systematic variation is observed. On many of the multiple crossings it is seen that the current magnitudes differ slightly on adjacent passes. This may be due to incomplete traversals. The vector directions on multiple passes appear to be fairly consistent. There appears to be a tendency for the currents observed from the few crossings in the dusk half of the tail (Y_{sm} positive) to have a small component towards the solar direction.

Normal Component

Some theories of the solar wind - magnetosphere interaction require little or no connection of polar magnetic field lines across the neutral surface in the tail (Dessler and Juday, 1965). In the region away from the diffusion region, Petschek (1964) requires a rather large, somewhat uniform normal component, and in the diffusion region Dungey (1958) and Speiser (1965) require a normal component which becomes weaker as the neutral point is approached. Speiser in fact, requires a normal component within the neutral sheet of about 1 gamma to produce auroral protons from the tail and only about 0.01 gamma to produce auroral electrons from the tail. This normal component has been measured for the 42 crossings as the value of B_z (average) at the time when B_x (average) goes to zero. ("Average" meaning the straight line approximation to the component data on crossing the sheet. See Figures 6 and 7.)

Figure 9 is a plot of the normal field components measured as described above versus (x, y) sm in the magnetospheric tail. The error bars are about $\pm 1/2\gamma$, coming partly from the known accuracy of each data point, and partly from the analyses used to obtain the measuring points. Orbit 39 appears to have an anomalously large normal component. Anderson and Ness (Figure 9, 1966) indicate a fairly high tail field over most of Orbit 39, and the cusp region appears to be much closer to the earth than usual. From Figure 8, it is seen that the current on orbit 39 also appears somewhat anomalous. The magnitude

is somewhat larger than those nearby and the direction more closely resembles the first four crossings. Magnetic activity as measured by a K_p index of 3 at this time may be responsible for these anomalous results.

Figure 9 also suggests that the strength of the normal component in the neutral sheet decreases near the noon-midnight meridian plane, as well as with increasing geocentric distance. Farther back in the tail and toward the evening side there is some indication of a weak southward normal component. However, from the accuracy of these analyses, all that can be said is that the normal field is very weak near the noon-midnight meridian plane ($B_z \leq 1\gamma$). If a neutral point or line, due either to reconnection or a sheet pinch, had been crossed, then one would expect the southward component to be systematically larger with distance from the zero field region.

The magnitude of the magnetic field outside of the current sheet is about the same across the tail. This can be seen from Figure 8 since the magnitude of the current is about the same across the tail. Therefore, an increased normal component toward the dawn side implies a larger field line curvature at the sheet and thus qualitatively implies a sheet which is thicker toward dawn than midnight. The magnitude of the magnetic field goes through a minimum on every sheet crossing, although it does not necessarily go to zero (see Figure 9.) This seems to rule out the possibility that the observed field reversals are purely rotational discontinuities.

Sheet Velocities and Thicknesses

As previously described, the relative velocity between the sheet and satellite, V_z , can be determined if the sheet thickness is known. V_z is, given by

$$V_z = V_{z(\text{sat})} - V_{z(\text{sheet})}$$

where $V_{z(\text{sat})}$ is the z component of the satellite's velocity, and $V_{z(\text{sheet})}$ is the sheet's velocity. $V_{z(\text{sat})}$ is known at a given time from the IMP-1 orbital parameters. $V_{z(\text{sheet})}$ can therefore be determined for assumed sheet thicknesses. Figure 10 shows the results plotted versus geocentric distance for an assumed sheet thickness of 500 km and 5000 km. For a thickness of 500 km, the average sheet velocity is about 0.1 km/sec for geocentric distances beyond $25 R_e$, and about 0.7 km/sec for distances less than $25 R_e$. For $Y = 5000$ km, the average sheet velocity at distances less than $25 R_e$ is about .2 km/sec and it is about -1.6 km/sec for distances greater than $25 R_e$. If one assumes that on a large number of passes the average sheet velocity observed should be about zero, then this plot suggests that the neutral sheet is thinner beyond $25 R_e$ than it is for geocentric distances less than $25 R_e$. Comparing Figure 8 or 9, it is seen that most of the crossings at geocentric distances less than $25 R_e$ occur toward

the dawn side of the tail. The interpretation can therefore also be made that the sheet appears to be thicker toward the dawn side of the tail than near the noon-midnight meridian plane. It is difficult from this statistical argument to distinguish between these two interpretations. However, if the argument from the previous section is used relating field line curvature through the sheet to sheet thickness, then, with Figure 9 it would appear that the change in sheet thickness is across the tail, with no change detected down the tail for these IMP-1 measurements.

There may be more sheet crossings than indicated in the previous figures during this period of Imp-1. Some of the other possible choices for crossings do not have clear and complete changes in the sign of B_x for this analysis. For example, on orbit 34, there may be three other possible crossings near the one chosen but they are less clear. On orbit 39, the magnetic field varies much more than usual on crossing the sheet, with the magnitude changing from one 20 second data point to the next by as much as 10 gammas. Away from the sheet on either side, the field appears much quieter. Particle or plasma effects may certainly be of importance in this and other cases, but detailed correlations have not been made. The sheet appears to be in motion, coupled with possible plasma effects, in all of the cases observed, even in those cases which appear to be single crossings.

Summary

On orbits 30 through 47, while the IMP-1 satellite was imbedded within the Earth's magnetospheric tail, 42 observations have been made where the magnetic field reverses and goes through a minimum value. Of these observations the first four on orbits 30, 31, 32, and 33, which were within $15 R_e$ and near the dawn meridian, appear to have the character of "inflated" field lines within the magnetosphere and not extended into the magnetospheric tail. The remaining 38 observations are identified as crossings of a neutral sheet or current sheet separating regions of oppositely directed magnetic field in the magnetospheric tail. The crossing observed on orbit 39 may be an exception and may more properly fit into the category of magnetospheric, not tail, field lines. On many orbits multiple crossings are observed. That is the neutral sheet appears to move back and forth across the spacecraft several times. The neutral sheet is a relatively narrow region of field reversal found within a broad plasma sheet region.

One of the major observations that has been made in this study is that the neutral sheet is often, if not always, moving. The sheet velocity has a maximum of a few kilometers per second, with a maximum amplitude, assuming sinusoidal motion, of the order of an earth-radius. This is superimposed on the gross-motion of the sheet as the base of the sheet moves due to the wobbling of the dipole axis and its changing orientation with respect to the sun. The base of the

sheet appears to be near the magnetic equatorial plane at a geocentric distance of $10 \pm 3 R_E$.

The strength of the magnetic field normal to the sheet has been measured for the 42 observations. Knowledge of this magnetic field component might help distinguish between the "open" or "closed" tail field topologies. That is, a zero normal component would imply no field connection and a long "open" tail, (Dessler, 1964), while a weak normal component diminishing with distance and even reversing would imply the existence of a neutral point (Dungey, 1961) near the so-called diffusion region. The diffusion region is that region near the neutral point where magnetic field lines are broken and reconnected. The conductivity cannot be assumed infinite and the magnetic field lines diffuse through the plasma. A larger and more uniform normal component would be suggestive of Petschek's (1964) model away from the diffusion region.

For those observations with the character of magnetospheric, not tail, field lines, the normal component is about ten gammas. Beyond $15 R_E$, it appears that there is some connection through the current sheet toward the dawn side of the tail, with little or no connection near the noon-midnight meridian plane. The value of the normal component beyond $15 R_E$ and near the dawn edge of the tail is 1 to 4 gammas or 5 to 20% of the tail field. Near the noon-midnight meridian plane, the normal component is less than one gamma. Thus although some field line connection is evident toward the dawn side of the tail, these results appear

inconclusive for distinguishing between "open" and "closed" tail field topologies. It is of course possible that the field topology is sometimes "open" and sometimes "closed". Further measurements and local time correlations with ground magnetic observations will help to answer this question.

For these measurements, no correlation has been found between ground magnetic activity, as measured by ΣK_p for 6 hours before and after a crossing, and the number of multiple crossings. The tail field magnitude remains about the same across the tail, so the increased normal component near the dawn side of the tail implies a larger radius of curvature of the field. Thus, qualitatively the sheet is thicker toward the dawn side of the tail than toward the noon-midnight meridian. This result agrees with the independent measurements of the sheet velocity. Assuming that the sheet velocity observed should be on the average zero, an average sheet thickness is determined. This thickness is larger close to the Earth and the dawn side of the tail, and smaller farther away and toward the noon-midnight meridian. This interpretation appears to be in agreement with the measurements of electrons by the Vela satellite in the plasma sheet (Bame et al., 1966) and by Imp-1 (Murayama, 1966).

References

Anderson, K. A., and N. F. Ness, Correlations of magnetic fields and energetic electrons on the IMP-1 satellite, to be published, 1966.

Bame, S. J., J. R. Asbridge, H. E. Felthouser, E. W. Hones, Jr., and I. B. Strong, Characteristics of the electrons in the plasma sheet of the magnetospheric tail, Trans. Am. Geophys. Union, 47, 141, March 1966.

Behannon, K. W., and N. F. Ness, Magnetic storms in the earth's magnetic tail, J. Geophys. Res., 71 (9), 2327, May 1966.

Dessler, A. J., The length of the magnetospheric tail, J. Geophys. Res., 69, 3913, 1964.

Dessler, A. J., and R. D. Juday, Configuration of auroral radiation in space, Planetary Space Sci., 13, 63-72, 1965.

Dungey, J. W., Conditions for the occurrence of electrical discharges in astrophysical systems, Phil. Mag., 44, 725, July 1953.

Dungey, J. W., Cosmic Electrodynamics, Cambridge University Press, Cambridge, 1958.

Dungey, J. W., Interplanetary magnetic field and the auroral zones, Phys. Rev. Letters, 6 (2), 47, January 1961.

- Giovanelli, R. G., Electric phenomena associated with sunspots, Monthly Notices Roy. Astron. Soc., 107, 338, 1947.
- Hoyle, F., Some Recent Researches in Solar Physics, Cambridge University Press, Cambridge, 1949.
- Ness, N. F., The earth's magnetic tail, J. Geophys. Res., 70, 2989-3005, 1965.
- Ness, N. F., and D. J. Williams, Correlated magnetic tail and radiation belt observations, J. Geophys. Res., 71 (1), 322, January 1966.
- Petschek, H. E., Magnetic field annihilation, in: AAS-NASA Symp. on the Physics of Solar Flares, ed. by W. N. Hess, Washington, D. C., NASA, (NASA SP-50), pp. 425-439, 1964.
- Serlemitsos, P., Low energy electrons in the dark magnetosphere, J. Geophys. Res., 71 (1), 61, January 1966.
- Speiser, T. W., Particle trajectories in model current sheets, 1. analytical solutions, J. Geophys. Res., 70 (17), 4219, Sept. 1, 1965
- Williams, D. J., and N. F. Ness, Simultaneous Trapped Electron and Magnetic Tail Field Observations, submitted to J. Geophys. Res., 1966.

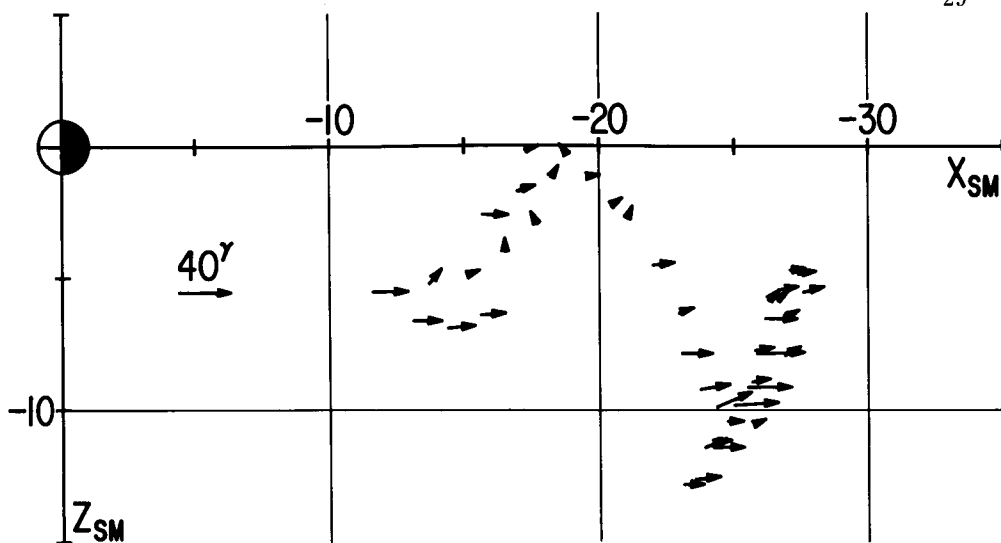
Figure Captions

- Figure 1 Summary of IMP-1 Magnetic field measurements in the magnetospheric tail. Vectors are hourly average, even hours only, projected onto planes of constant Y_{sm} (solar-magnetospheric) for measurements within the indicated ranges of Y_{sm} .
- Figure 2 Summary of IMP-1 Magnetic field measurements in the magnetospheric tail. (See Figure 1 caption.)
- Figure 3 Summary of IMP-1 Magnetic field measurements in the magnetospheric tail. (See Figure 1 caption.)
- Figure 4 Perpendicular distances from the solar-magnetospheric (Z_{sm}) and magnetic (Z_{mag}) equatorial planes where neutral sheet crossings were observed with the IMP-1 satellite. Orbit numbers and χ_{ss} , the magnetic latitude of the sub-solar point, are given for each crossing.
- Figure 5 Possible neutral surface and tail field configuration for a large value of χ_{ss} , in the noon-midnight meridian plane. The corresponding orbit numbers and crossing positions from Figure 4 are indicated. The hourly averaged vector measurements for $-1 < Y_{sm} < +1$ from Figure 3 are superimposed. (See text.)

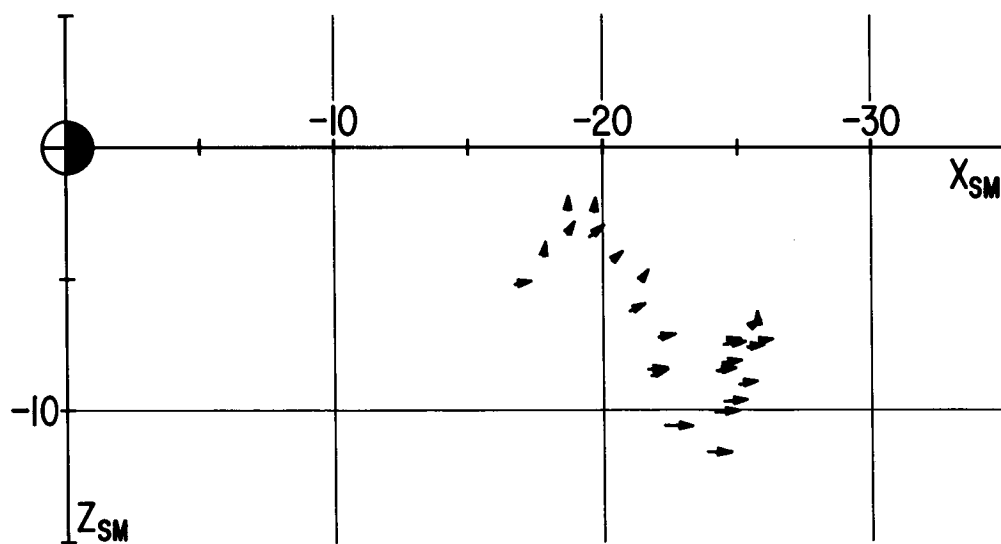
- Figure 6 Solar-Magnetospheric magnetic field components and total field (\bar{F}) versus time for the neutral sheet crossings on orbit 45 near $26 R_E$. A straight line approximation (dashed lines) is made for the components at each sheet crossing, and used to determine the equivalent current density. Note the five crossings, i.e. field reversals accompanied by a minimum in the total field, and the traversal times. Vertical lines indicate the times at which the average of B_x is zero, and the sheet normal component, B_z , is measured at those times.
- Figure 7 Solar-Magnetospheric magnetic field components and total field (\bar{F}) versus time for the interval of field reversal on orbit 32. Notice the large normal field component, about 10 gammas, and the large change in B_y as well as B_x as the sheet is traversed.
- Figure 8 Equivalent current per unit length from curl \mathbf{B} for the indicated orbits versus (X - Y) solar-magnetospheric crossing positions. Note the multiple crossings as on orbit 45 at about $26 R_E$ (compare Figure 6). (See text.)

Figure 9 Normal magnetic field component within the sheet for the 42 observations. B_z positive is northward, the direction of a dipole field line at the magnetic equatorial plane. The error bars from the analysis are about $\pm 1/2 \gamma$.

Figure 10 Neutral sheet velocities for an assumed thickness of 500 km or 5000 km plotted versus geocentric distance for the 42 observed crossings. (See text.)



$$-16 < Y_{SM} < -13$$



$$-25 < Y_{SM} < -16$$

Figure 1

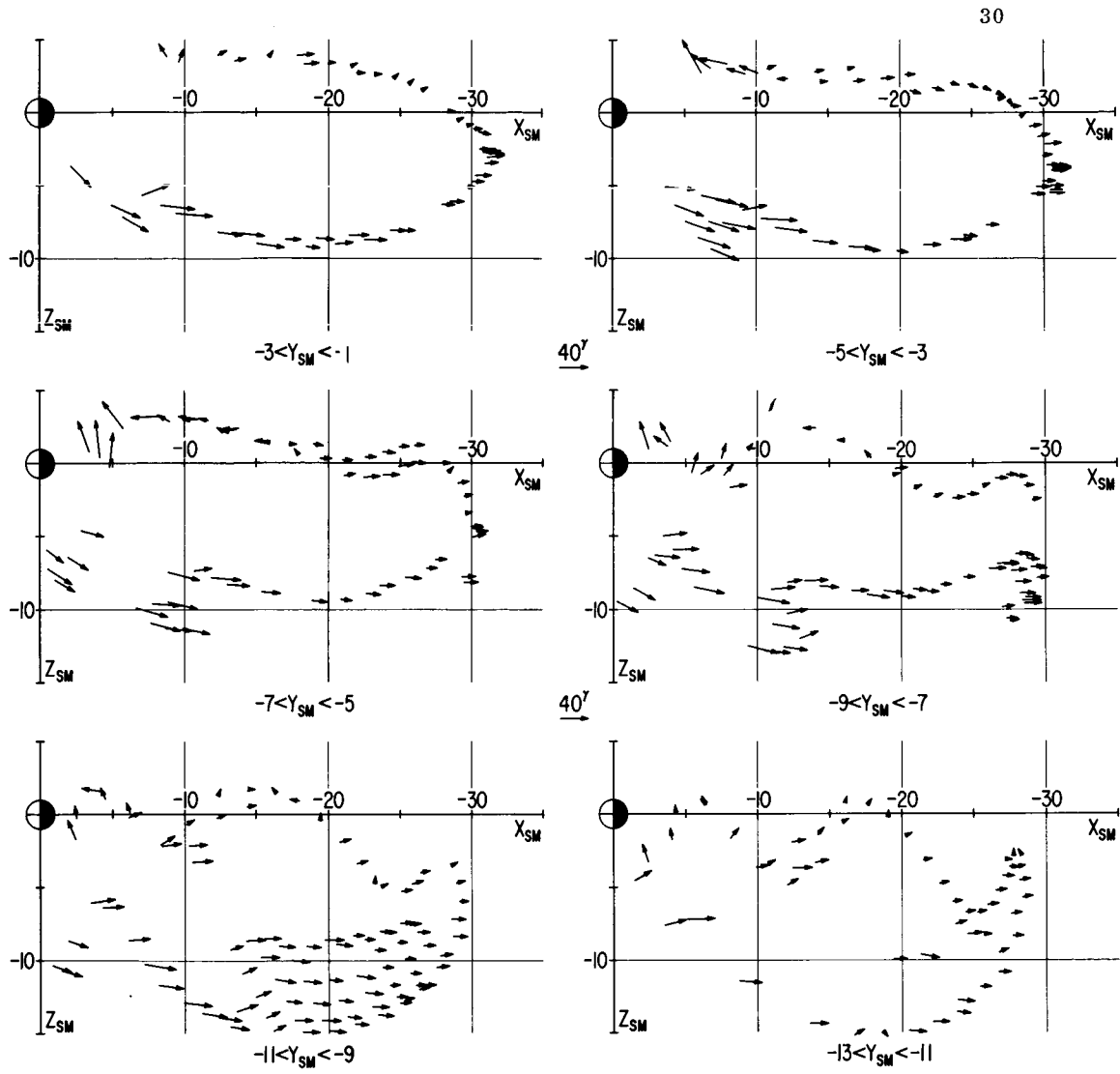


Figure 2

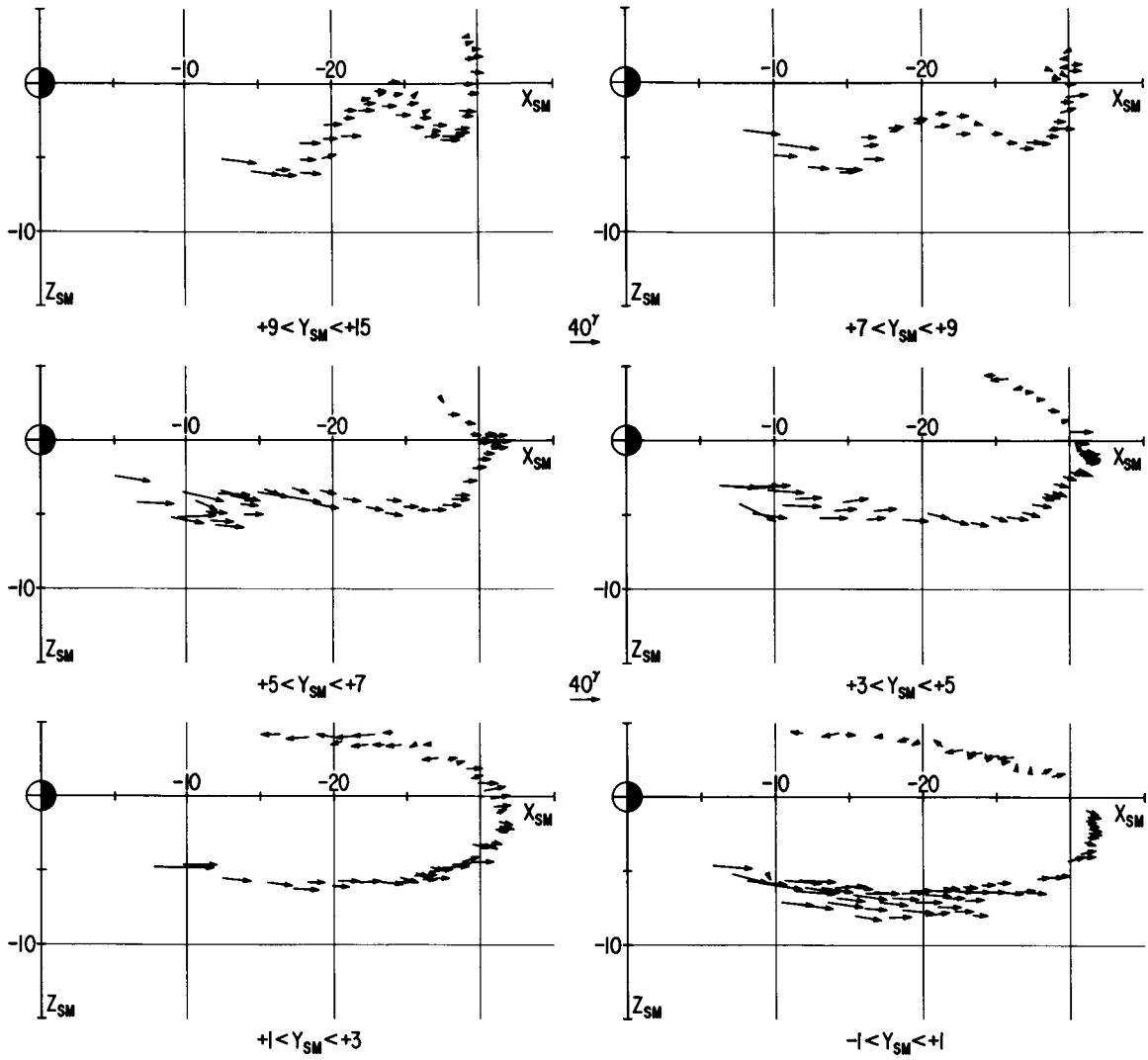


Figure 3

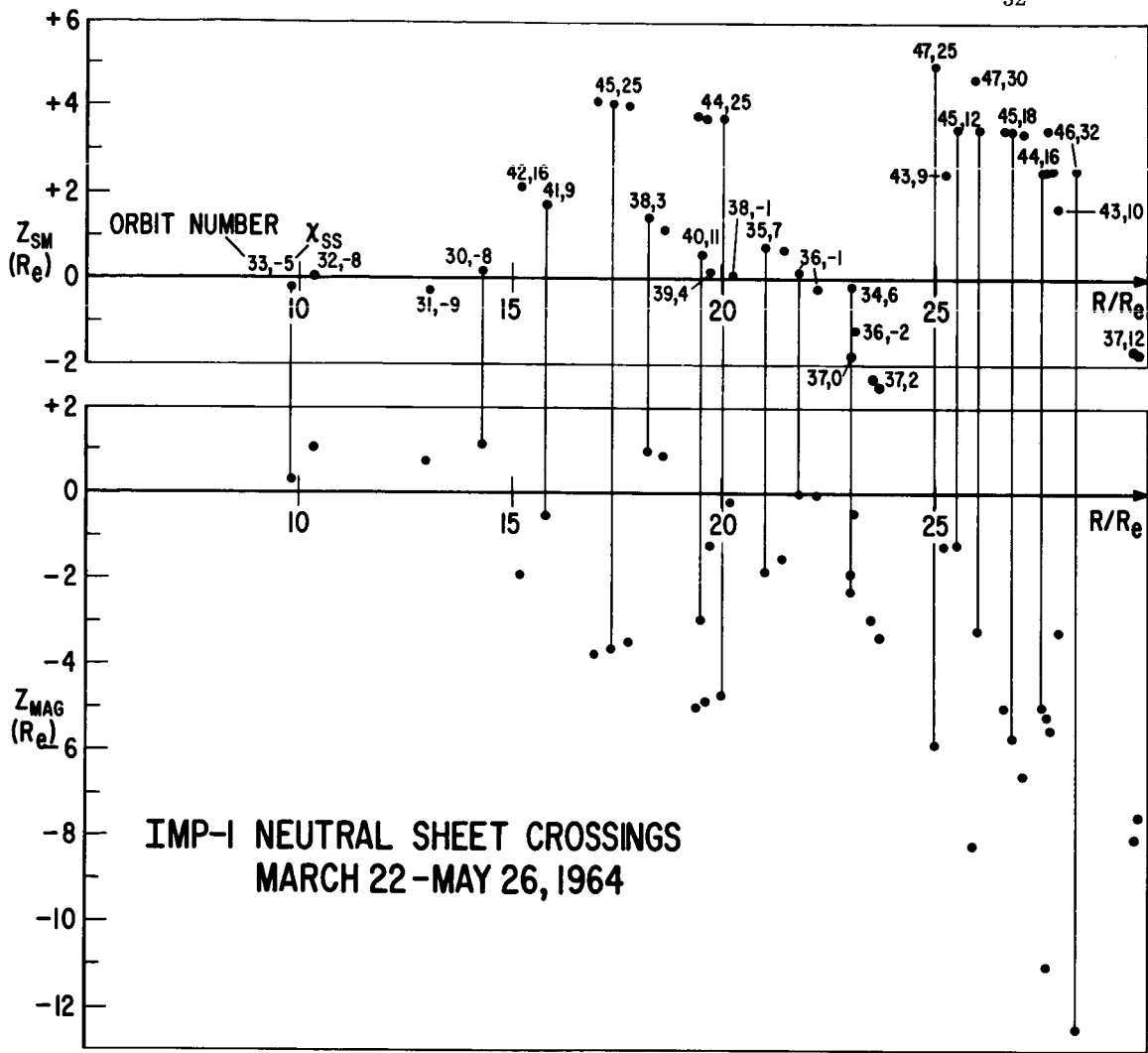


Figure 4

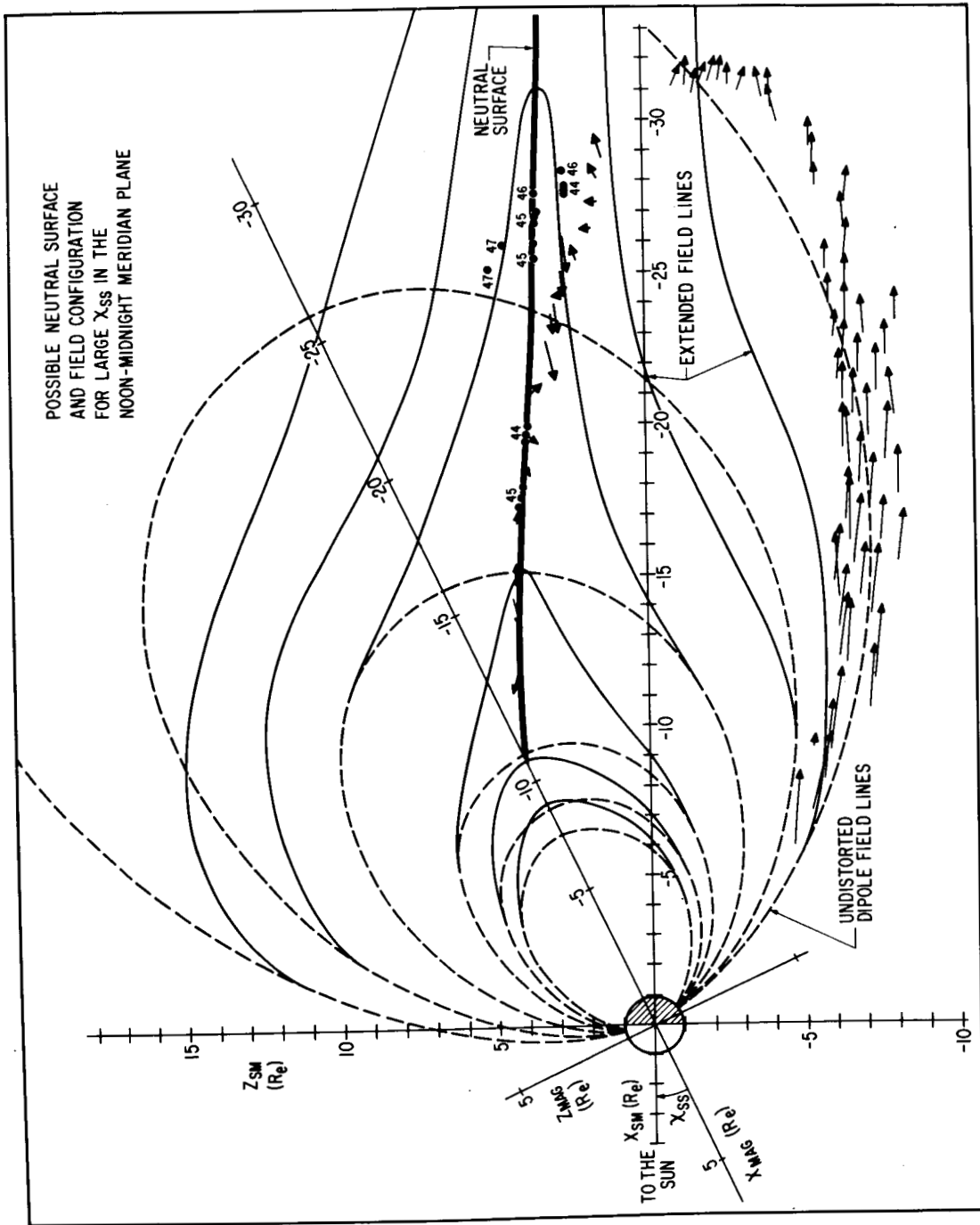


Figure 5

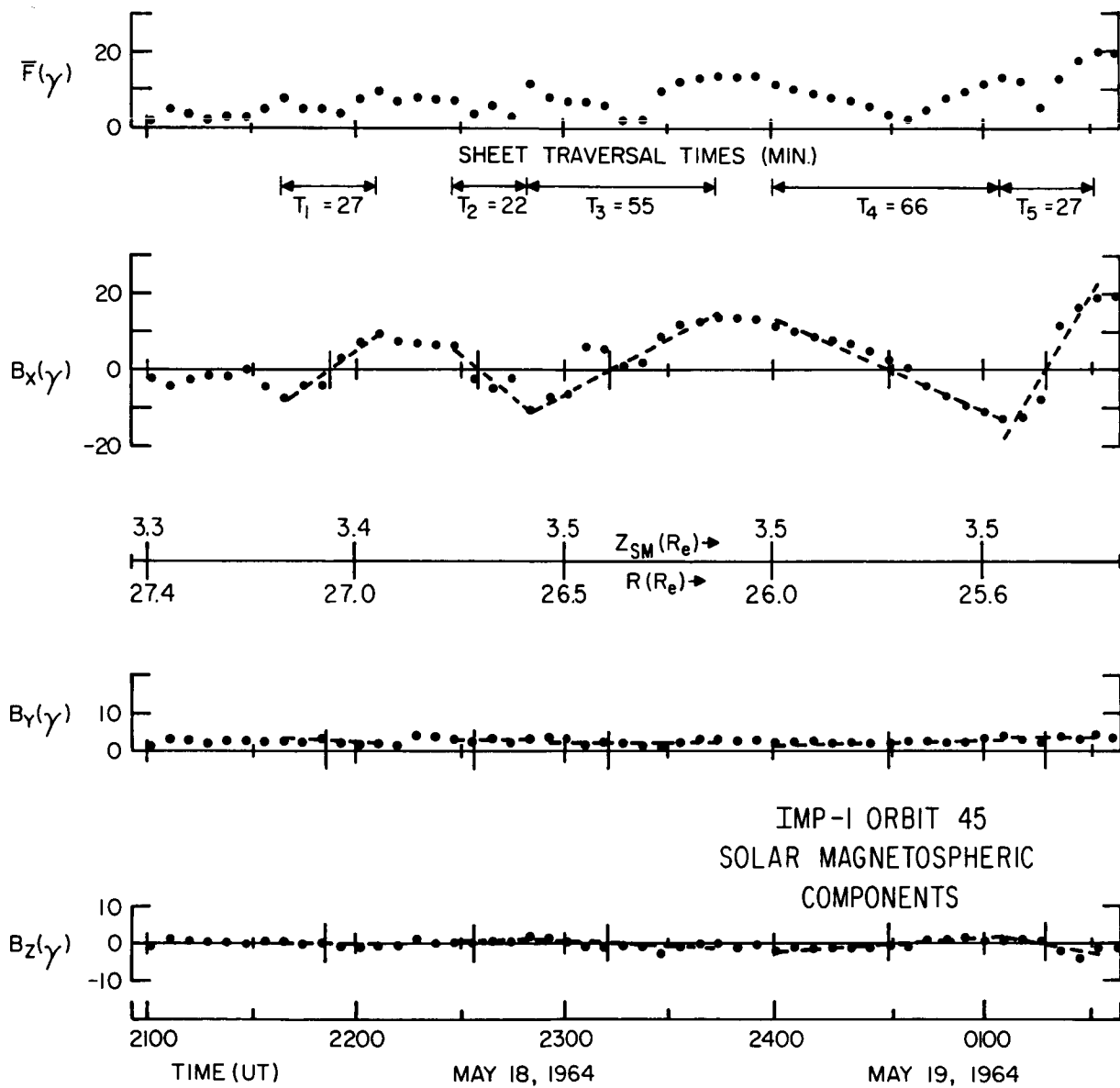


Figure 6

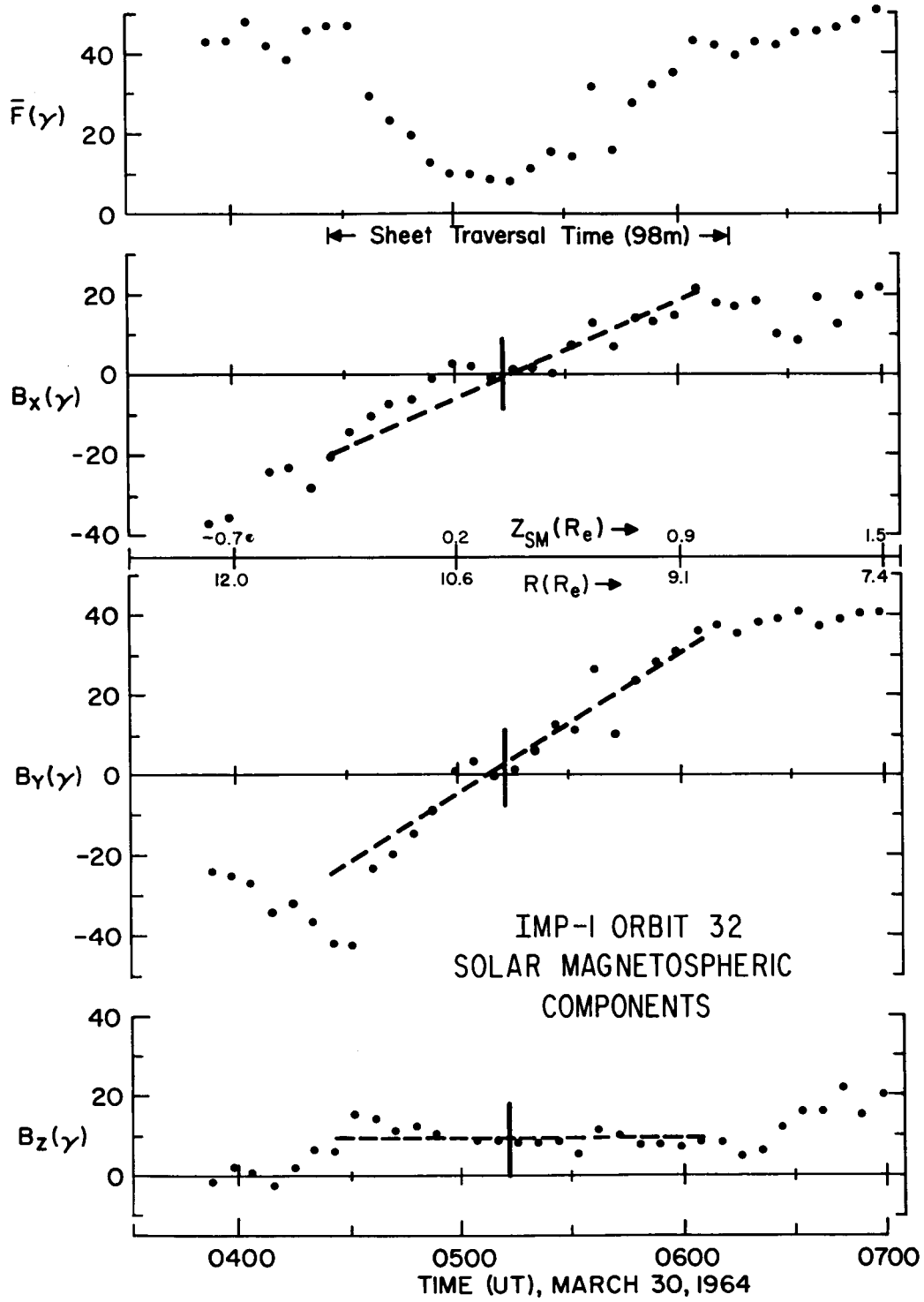


Figure 7

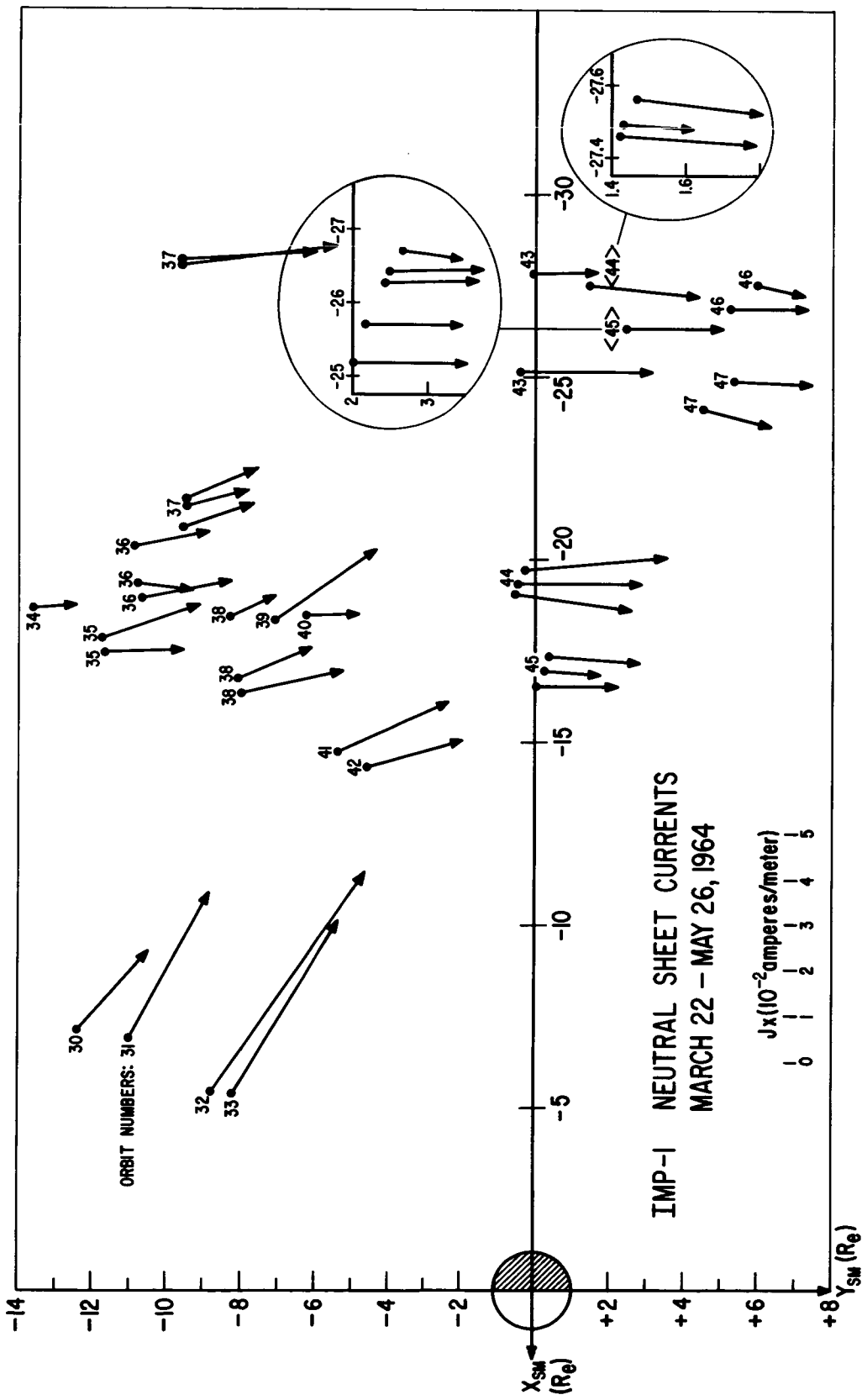


Figure 8

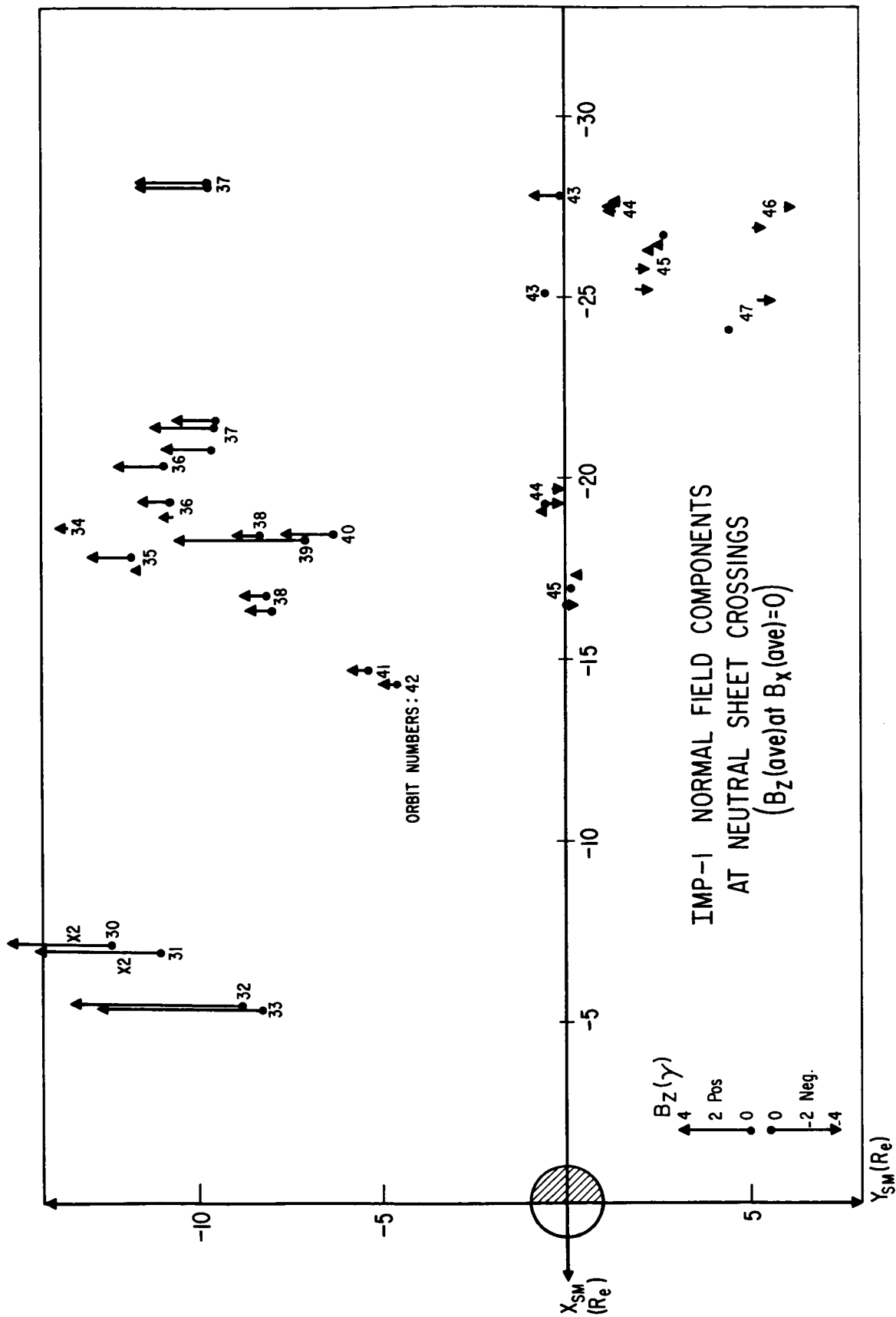


Figure 9

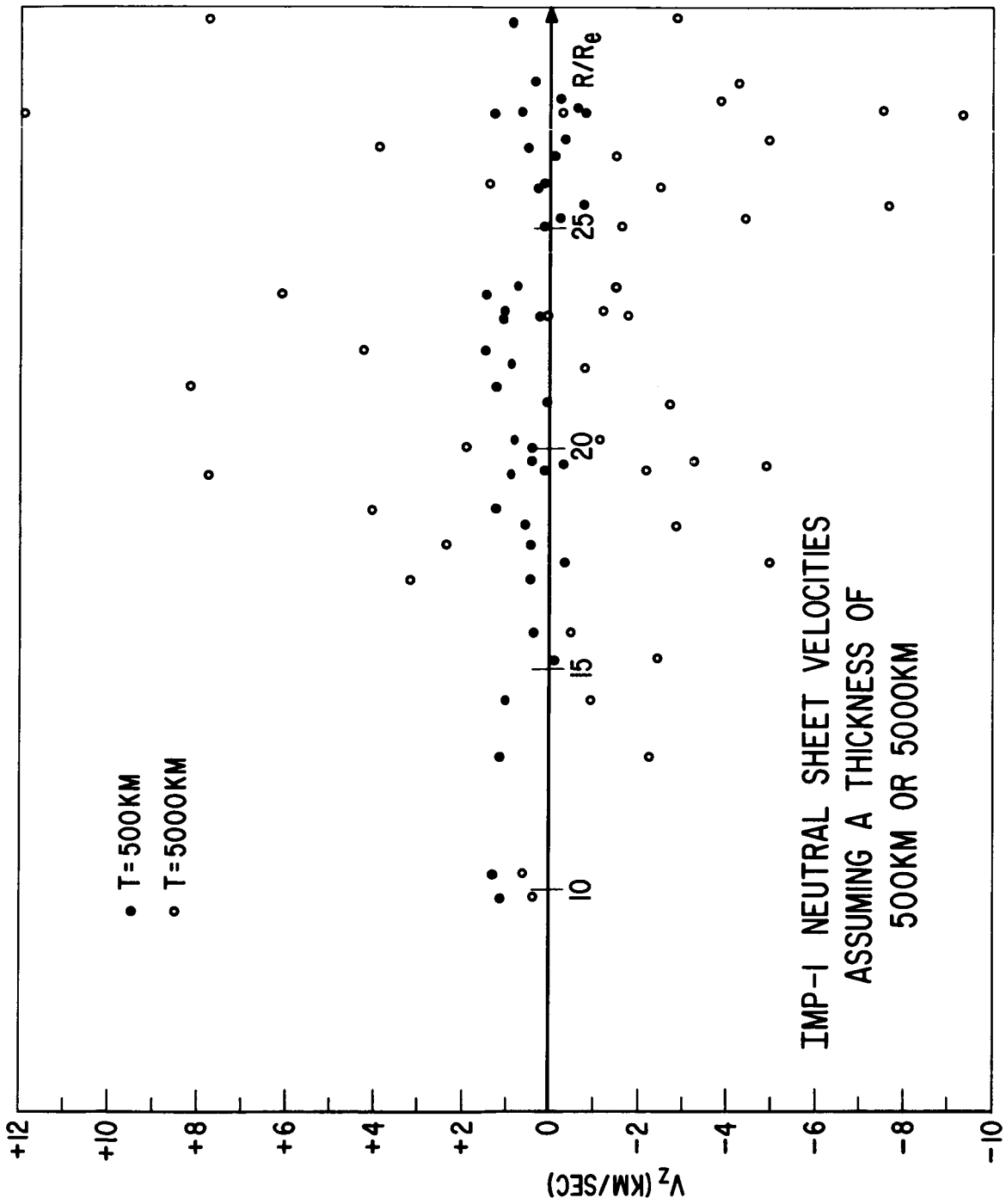


Figure 10